Journal of Materials Chemistry

Cite this: *J. Mater. Chem.*, 2011, **21**, 16442

www.rsc.org/materials

PAPER

Diazaboroles with quinone units: hydrogen bonding network and n-type FETs involving a three-coordinate boron atom†

Jun-ichi Nishida,[a] Tomohiro Fujita,[a] Yoshihide Fujisaki,[b] Shizuo Tokito[b] and Yoshiro Yamashita*[a]

Received 9th June 2011, Accepted 22nd August 2011
DOI: 10.1039/c1jm12650d

A series of monodiazaborole and bis(diazaborole) derivatives with a quinone moiety have been prepared as stable electron acceptors. They show dark colors in the solid states and reversible reduction potentials in the cyclic voltammograms. X-Ray structure analysis of one derivative revealed a π-stacking structure accompanied with a hydrogen-bonding network. Trifluoromethyl substituted derivatives afforded n-type FET characteristics with an electron mobility of 10^{-2} cm^2 V^{-1} s^{-1}. An ambipolar FET characteristic was also observed in the biphenyl derivative. The planar three-coordinate boron units were used as π-linkers to afford n-type and ambipolar FET characteristics.

Introduction

Development of organic materials for transporting electrons has recently attracted much attention because they can be applied to n-type semiconductors for organic electronic devices such as field-effect transistors (FETs) and organic photo-voltaic cells (OPVCs).[1,2] In this field, organic π-systems containing a three-coordinate boron atom are of interest since the boron atom has a planar geometry with a vacant p-orbital and can connect π-conjugated systems.[3–8] Among them, the derivatives including boron–nitrogen bonds are known to be stable by a flow of lone-pair electrons of nitrogen to the vacant p-orbital of boron.[5–8] Since they do not need bulky substituents for stabilization, strong intermolecular interactions helpful for fast carrier transportation can be expected. However, such π-systems generally show high HOMO levels[8] and have not been applied to n-type semiconductors for FETs. Bearing this in mind, new three-coordinate boron derivatives **1–3** based on 1,3-diazaboroles[7,8] and quinone units[9] have been synthesized. They have the following advantages. First, they have high electron-accepting properties. Quinone units attract the lone-pair electrons of the nitrogen, and the empty p_z orbital of boron is expected to work for transporting electrons. Second, they have higher symmetrical structures compared with isoelectronic pyrrole derivatives. Even in the asymmetrical monodiazaborole derivatives **1** and **2** (Fig. 1), a C2-axis remains along with the molecular long axis. Third, they contain proton donor and acceptor units. Well-ordered molecular arrangements through hydrogen bonds are expected. Fourth, they are easily prepared by a one-pot condensation reaction and stable enough to handle in air. The physical properties can be controlled by modification of boronic acids and quinone moieties as shown in compound **2**. We report here the first examples of n-type and ambipolar

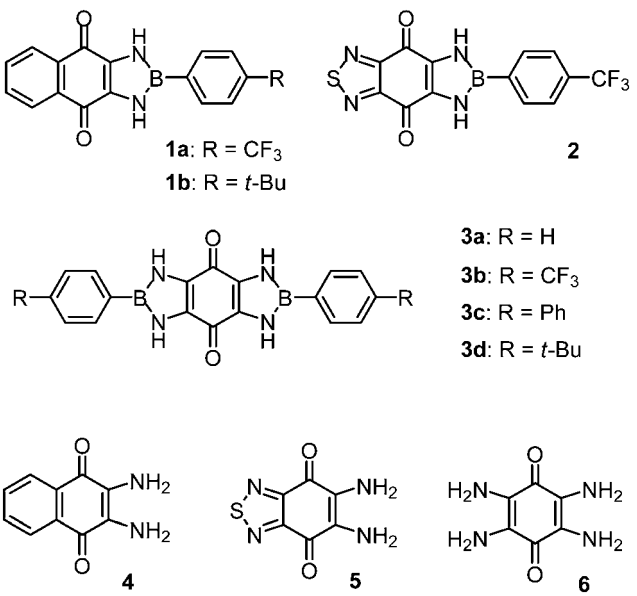

Fig. 1 Chemical structures of monodiazaborole derivatives **1** and **2**, bis(diazaborole) derivatives **3**, and their amine precursors.

[a]*Department of Electronic Chemistry, Interdisciplinary Graduate School of Science and Engineering, Tokyo Institute of Technology, 4259 Nagatsuta, Midori-ku, Yokohama, 226-8502, Japan. E-mail: yoshiro@echem.titech.ac.jp; Fax: +81-45-924-5489; Tel: +81-45-924-5571*
[b]*NHK Science & Technical Research Laboratories, Kinuta, Setagaya-ku, Tokyo, 157-8510, Japan*

† Electronic supplementary information (ESI) available: FT-IR data, NMR data, X-ray analysis, reflection spectra after K–M transformation, DPV data, molecular orbital calculations of the compounds and the tautomeric and dimer forms of **1a**, FET, XRD and AFM data. CCDC reference number 819166. For ESI and crystallographic data in CIF or other electronic format see DOI: 10.1039/c1jm12650d

FETs based on planar crystalline three-coordinate boron derivatives.[10]

Results and discussion

Synthesis and characterization

Monodiazaborole- and bis(diazaborole)–quinone derivatives **1–3** were prepared by the condensation reaction of diaminoquinones **4** and **5** (ref. 11) or tetraaminoquinone **6** with the corresponding boronic acids **7** in toluene. Compounds **1b** and **3d** with *tert*-butyl groups were prepared to increase the solubility. These compounds were purified by sublimation (yields after sublimation: **1a** 48%, **1b** 54%, **2** 35%, **3a** 19%, **3b** 54%, **3c** 4%, **3d** 12%), and characterized by MS and elemental analysis.

Photophysical properties

The absorption maxima of monodiazaborole derivatives **1a** and **1b** were observed at 290, 456 and 286, 471 nm in DMF, respectively (Fig. 2 and Table 1). Compound **2** with a thiadiazole ring showed a similar absorption spectrum and is pale yellow in solution. On the other hand, the absorption maxima of bis(diazaborole) derivatives **3a–d** were observed at 348, 321, 319 and 353 nm, respectively, which are almost colorless in solution. The result observed in **3** suggests that π-conjugation based on 1,3-diazaborole rings is not effective for the red-shift of absorption in solution. On the other hand, in the solid state, these compounds show dark color (**1** and **2**: dark red, **3**: dark brown). Reflection spectra of **1a**, **2** and **3b** in the solid state are collected by using an integrated sphere and depicted in Fig. 3. While **1a** and **2** effectively reflect the light at longer wavelengths (>600 nm), almost all visible light is absorbed in compound **3b**. These are attributed to the intra- and intermolecular charge-transfer and a hydrogen-bonding network between the diazaborole and quinone units.

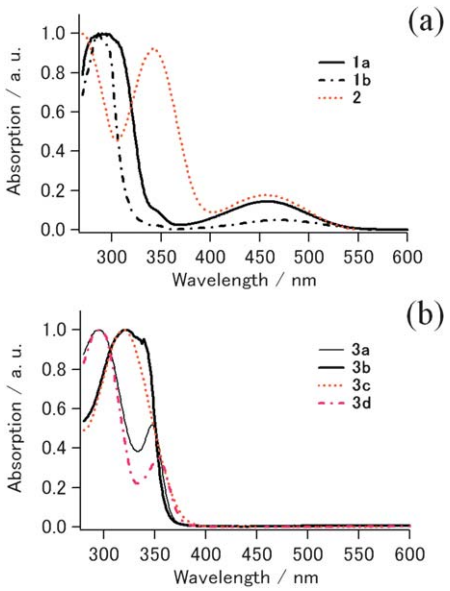

Fig. 2 UV-Vis spectra of (a) monodiazaborole derivatives **1** and **2**, and (b) bis(diazaborole) derivatives **3** in DMF.

Table 1 Optical and electrochemical data

Compound	λ_{abs}[a]/nm (log ε)	E_{pc}[b]/V	E_{pa}[b]/V	LUMO[f]
1a	290, 456	−0.93, −1.04[c]		3.44
1b	286 (4.64), 471 (3.32)	−0.84[c]	+1.33[d]	3.48
2	271, 342, 458	−0.66[c]		3.71
3a	294, 348	−0.91[e]	+0.83[e]	3.46
3b	274, 321	−0.86[e]	+0.91[e]	3.51
3c	269, 319	−0.91[e]	+0.85[e]	3.46
3d	293 (4.62), 353 (4.12), 596 (2.28)	−0.97[c]	+0.86[d]	3.40

[a] In DMF. [b] 0.1 M n-Bu_4NPF_6 in DMF, Pt electrode, V *vs.* SCE. [c] CVs, reversible waves, half-wave potentials. [d] CV, irreversible wave, peak potential. [e] DPVs, peak potentials. [f] Calculated from reduction potentials.

Electrochemical properties

These compounds have electron-accepting properties attributed to the quinone units. The reduction potentials were measured by cyclic voltammograms (CV) and differential pulse voltammograms (DPV) and the results are summarized in Table 1. The naphthoquinone derivatives **1a** and **1b** showed reversible reduction peaks in the CVs (Fig. 4a and b). Replacement of the fused benzene ring with a thiadiazole one in **2** decreases the LUMO level, whose reduction potential was observed at −0.66 V. Because of the poor solubility of bis(diazaborole) derivatives **3a–c**, their reduction potentials were determined by DPVs. A CV of a compound **3d** with *tert*-butyl groups could be measured and showed a reversible reduction peak and an irreversible oxidation peak as depicted in Fig. 4d. Oxidation peaks were observed in all of derivatives **3** and **1b**.

X-Ray structure analysis

A single crystal of compound **1a** was obtained from slow sublimation.‡ X-Ray analysis revealed the planar geometry with a dihedral angle of 4.8° between the diazaborole and phenyl rings. Interestingly, an infinite one-dimensional hydrogen-bonding network was observed between the hydrogen atoms of

‡ X-Ray measurement of single crystal of **1a** was carried out using a RAXIS-RAPID imaging plate diffractometer with Mo-Kα radiation (λ = 0.71075 Å) at −180.0 °C. The structure was solved by the direct method (SIR2004) and refined by the full-matrix least-squares method on F^2. The non-hydrogen atoms were refined anisotropically. Hydrogen atoms were refined using the riding model. Absorption correction was applied using an empirical procedure. All calculations were performed using the crystal structure crystallographic software package except for refinement, which was performed using SHELXL-97.
Crystal data for ***1a***: $C_{17}H_{10}N_2O_2F_3B_2$, M = 342.08, red platelet, crystal dimensions 0.70 × 0.70 × 0.15 mm, triclinic, space group $P\bar{1}$, a = 5.5337 (12), b = 7.9622(19), c = 16.321(3) Å, α = 101.835(6), β = 94.236(7), γ = 93.967(6), V = 699.3(3) Å^3, Z = 2, D_c = 1.625 g cm^{-3}, 6507 reflections collected, 3115 independent (R_{int} = 0.049), GOF = 1.022, R_1 = 0.1265 ($I > 2.00\sigma(I)$), wR_2 = 0.3359 for all reflections. The CCDC reference number is 819166.

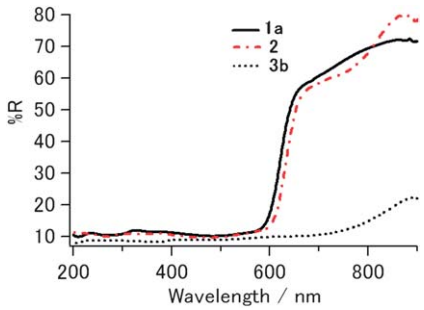

Fig. 3 Reflection spectra of **1a**, **2** and **3b** in the solid state.

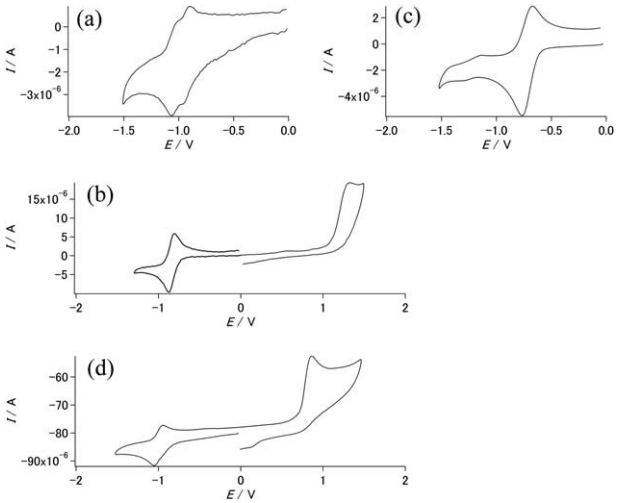

Fig. 4 Cyclic voltammograms of (a) **1a**, (b) **1b**, (c) **2**, and (d) **3d**.

the diazaborole and oxygen atoms of the quinone unit (2.09 Å) as shown in Fig. 5. A π-stacking structure is formed between the networks with an interplanar distance of 3.41 Å, in which a short contact of 3.15 Å between the carbonyl groups was observed. The π-stacking structure suggests the formation of a channel for electron transportation through the LUMO. The HOMOs and LUMOs are estimated by the molecular orbital calculations based on the B3LYP/6-31G(d) level of theory (Fig. 6a). To investigate a possibility of hydrogen transfer, tautomeric forms **1a**-B, **1a**-C (Fig. 6b) and a dimer model were also calculated

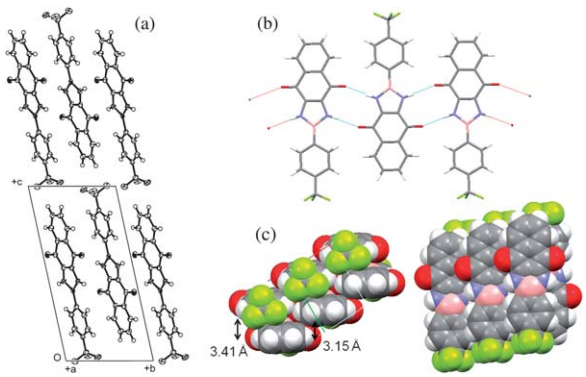

Fig. 5 (a) Crystal packing of **1a** viewed along the *a*-axis, (b) the hydrogen-bonding network and (c) overlapping modes.

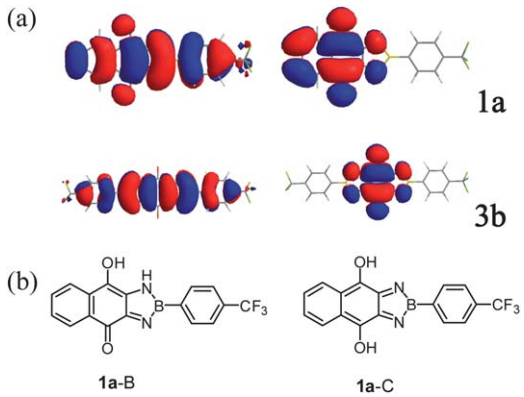

Fig. 6 (a) HOMO (left) and LUMO (right) of **1a** and **3b** calculated from the B3LYP/6-31G(d) level of theory. (b) Tautomeric forms of **1a**-B and **1a**-C.

(Fig. S6 and Tables S1 and S2 in the ESI†). Although the tautomeric forms have high single point energies compared with **1a** (**1a**-B: Δ38.8 kcal mol^{-1}, **1a**-C: Δ80.7 kcal mol^{-1}), their small HOMO–LUMO energies may contribute to the red-shift of the absorption in the solid state. The similar hydrogen-bonding networks are observed in compounds **1b** and **2** in their FT-IR data (Fig. S1 in the ESI†).

FET characteristics

The FET devices based on them were fabricated on thermally oxidized silicon oxide with bottom-contact configuration, and the measurements were carried out *in situ* without exposure to air. A monodiazaborole derivative **1a** showed clear n-type FET characteristics with an electron mobility of 3.9×10^{-2} cm^2 V^{-1} s^{-1} and a high on/off ratio of 10^6 (Table 2). Similar n-type characteristics were observed for compound **2** with an electron-accepting thiadiazole. Unfortunately, in air, the n-type performances gradually decreased (see ESI†). To improve the air stability, higher electron accepting heterocycles are necessary. In the case of symmetrical bis(diazaborole) derivatives **3**, **3b** with trifluoromethyl groups exhibited good n-type behavior although unsubstituted phenyl derivative **3a** did not show FET characteristics. This result indicates that the trifluoromethyl group is necessary to show efficient n-type FET behavior.[9d] On the other hand, compound **3c** containing biphenyl units provided ambipolar FET characteristics.

Table 2 FET characteristics with bottom contact geometries[a]

Compound	T_{sub}/ degree	Mobility/ cm^2 V^{-1} s^{-1}	On/ off	Threshold/ V
1a	20	n: 8.8×10^{-3}	4×10^6	+49
	100	n: 3.9×10^{-2}	1×10^6	+53
2	20	n: 3.7×10^{-2}	6×10^5	+38
3b	20	n: 1.5×10^{-2}	3×10^3	+43
	50	n: 9.2×10^{-3}	1×10^5	+39
3c	20	n: 2.3×10^{-5}	7×10^3	+53
	20	p: 1.5×10^{-5}	6×10	−75

[a] SiO_2 gate dielectric: 300 nm thick. HMDS treated surface. Interdigitated gold source and drain electrodes, L/W: 25 μm/294 mm.

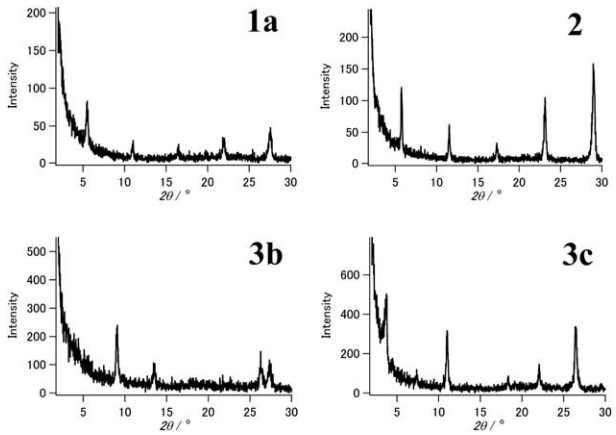

Fig. 7 X-Ray diffractograms of films **1a** (T_{sub} = 100 °C), **2** (20 °C), **3b** (20 °C) and **3c** (20 °C) on HMDS treated surfaces.

XRD analysis and AFM measurements

The thin films of **1–3** were examined by X-ray diffraction in reflection mode (XRD). XRD patterns of films **1a**, **2**, **3b** and **3c** are shown in Fig. 7. In the thin film of **1a**, reflections up to the fifth order were observed, indicating formation of lamellar ordering and high crystallinity on the substrate. The *d*-spacing calculated from the first reflection peak is 16.6 Å. Since the molecular length estimated from the X-ray analysis is 14.4 Å, **1a** is considered to stand perpendicularly to the substrate. Compound **2** also showed similar reflections up to the fifth order, indicating the perpendicular molecular arrangement (*d*-spacing: 15.4 Å). On the other hand, in the case of symmetrical bis(diazaborole) derivatives **3**, the *d*-spacings estimated from the first reflection peaks of films **3a–c** were observed at 13.8, 19.5 and 23.5 Å respectively (Fig. 7 and ESI†), which are not corresponding to calculated molecular lengths (17.7 Å for **3a**, 18.6 Å for **3b**, and 26.3 Å for **3c**). Therefore, molecules of **3a–c** are considered to stand with declined orientation on the substrate and they gave more complicated XRD patterns. These results suggest that the hydrogen-bonding networks in monodiazaborole derivatives **1–2** are favorable to afford well-ordered crystalline films.

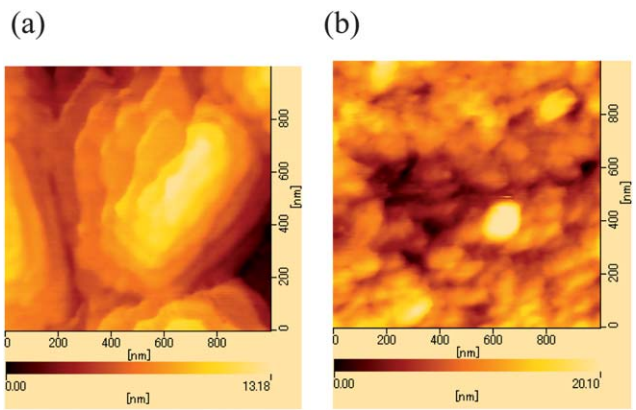

Fig. 8 AFM images of films (a) **1a** (T_{sub} = 100 °C) and (b) **3b** (20 °C) on HMDS treated surfaces.

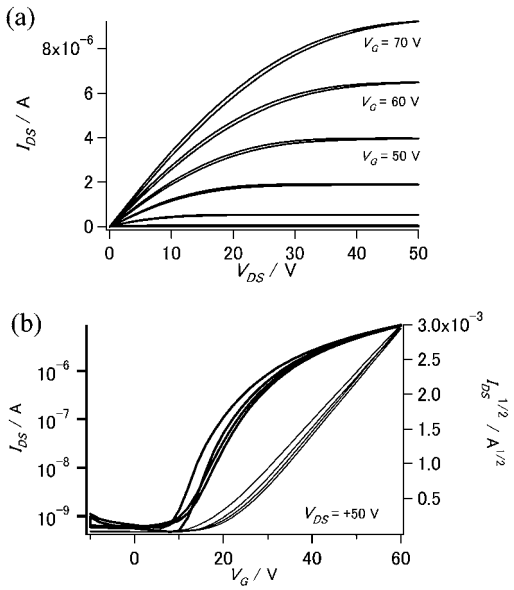

Fig. 9 Top-contact FET characteristics of **1a** (T_{sub} = 20 °C, HMDS treated surface): (a) output and (b) transfer characteristics.

AFM measurements and top-contact FET

To further study the film morphology, atomic force microscopy (AFM) images were measured with the tapping mode. AFM images of **1a** and **3b** showed flat surfaces and the surface of **1a** was smoother than that of **3b**. In the film **1a**, a stair-like layer with a vertical step size of *ca.* 1.6 nm corresponding to the molecular length was observed as depicted in Fig. 8a. This fact supports that the molecules stand on the substrate. A top-contact FET device of **1a** with a smooth surface was also fabricated. n-Type characteristics with an electron mobility of 0.04 cm^2 V^{-1} s^{-1}, on/off ratio of 10^6 and threshold voltage of +21 V were obtained. Output and transfer characteristics with small hysteresis are shown in Fig. 9.

Conclusions

In summary, we have developed novel π-systems composed of diazaboroles and quinones. The three-coordinate boron units having planar molecular geometries could be used as linkers of π-systems leading to high electron transportation. Although the calculated LUMOs are mainly localized on the quinone moieties, planar boron units effectively assist to afford the n-channels accompanied with well-ordered molecular arrangements. Further modifications of the electron-accepting parts are underway.

Experimental

General information

Melting points were obtained on a SHIMADZU DSC-60. ^{1}H-NMR spectra were recorded on a JEOL JNM-ECP 300 spectrometer. DI-MS data were collected on a JEOL JMS-700 mass spectrometer. IR spectra were recorded using a Smart iTR/ZnSe ATR on the Thermo SCIENTIFIC Nicolet iS10 FT-IR. UV-Vis spectra were recorded

on a SHIMADZU Multi Spec-1500 and a JASCO V-650 spectrophotometer. Reflection spectra in the solid states are collected by using a JASCO ISV-722 integrated sphere. Cyclic voltammograms and differential pulse voltammograms were recorded on a HOKUTODENKO HZ-5000. Pt disk, Pt wire and SCE were used as working, counter, and reference electrodes. Tetrabutylammonium hexafluorophosphate ($TBAPF_6$: 0.1 mol dm^{-3}) was used as supporting electrolyte in dry dimethylformamide (DMF). MO calculations were carried out by DFT methods at the B3LYP/6-31G(d) level using the Gaussian program 03. X-Ray diffraction (XRD) measurements were carried out on a Rigaku RINT with a CuKα source ($\lambda = 1.541$Å). AFM experiments for films in a tapping mode were performed using a SII NanoTechnology SPA-400 (DFM) instrument.

Materials

2-(4-Trifluoromethylphenyl)-2,3-dihydro-1*H*-1,3-diaza-2-bora-cyclopenta[*b*]naphthalene-4,9-dione (1a). A mixture of 4-(trifluoromethyl)phenylboronic acid **7b** (221 mg, 1.17 mmol) and 2,3-diaminonaphthoquinone **4** (200 mg, 1.06 mmol) in toluene (150 mL) was refluxed for 18 h. The resulting precipitate was filtered off while the solution was hot. Purification of the crude product by sublimation gave a reddish-brown solid of **1a** (174 mg, 48%).

Mp > 295 °C (decomp.). MS/EI (70 eV): *m*/*z* 342 (M^+, 100%). IR(KBr) ν (cm^{-1}): 3329, 1629, 1584, 1424, 1327, 1261, 1113, 1073, 972, 836, 751. Anal. calcd for $C_{17}H_{10}BF_3N_2O_2$: C, 59.69; H, 2.95; N, 8.19. Found: C, 59.74; H, 2.70; N, 8.20.

2-(4-*t*-Butylphenyl)-2,3-dihydro-1*H*-1,3-diaza-2-bora-cyclopenta[*b*]naphthalene-4,9-dione (1b). A mixture of 4-*tert*-butylphenylboronic acid **7d** (210 mg, 1.18 mmol) and 2,3-diaminonaphthoquinone **4** (200 mg, 1.06 mmol) in toluene (150 mL) was refluxed for 18 h. The resulting precipitate was filtered off while the solution was hot. Purification of the crude product by sublimation gave a reddish-brown solid of **1b** (190 mg, 54%).

Mp > 362 °C (decomp.). MS/EI (70 eV): *m*/*z* 330 (M^+, 100%). ^{1}H-NMR (300 MHz, DMSO): δ 10.17 (s, 2H, NH), 8.04 (d, 2H, J = 8.0 Hz), 7.99 (dd, 2H, J = 3.5, 3.5 Hz), 7.76 (dd, 2H, J = 3.5, 3.5 Hz), 7.41 (d, 2H, J = 8.0 Hz), 1.30 (s, 9H). IR(KBr) ν (cm^{-1}): 3329, 2957, 1634, 1587, 1456, 1425, 1408, 1256, 1200, 1151, 970, 765, 710. Anal. calcd for $C_{20}H_{19}BN_2O_2$: C, 72.75; H, 5.80; N, 8.48. Found: C, 72.80; H, 5.29; N, 8.62.

6-(4-Trifluoromethylphenyl)-6,7-dihydro-5*H*-2-thia-1,3,5,7-tetraaza-6-bora-*s*-indacene-4,8-dione (2). A mixture of 4-(trifluoromethyl)phenylboronic acid **7b** (213 mg, 1.12 mmol) and 2,3-diamino[5,6-*c*]thiadiazolequinone **5** (200 mg, 1.02 mmol) in toluene (150 mL) was refluxed for 18 h. The resulting precipitate was filtered off while the solution was hot. Purification of the crude product by sublimation gave a reddish-brown solid of **2** (125 mg, 35%).

Mp > 293 °C (decomp.). MS/EI (70 eV): *m*/*z* 350 (M^+, 100%). IR(KBr) ν (cm^{-1}): 3326, 1645, 1525, 1413, 1324, 1152, 1117, 1072, 1020, 846, 754. Anal. calcd for $C_{13}H_6F_3N_4O_2S$: C, 44.60; H, 1.73; N, 16.00; S, 9.16. Found: C, 44.55; H, 1.80; N, 15.98; S, 8.98.

2,6-Diphenyl-2,3,6,7-tetrahydro-1*H*,5*H*-1,3,5,7-tetraaza-2,6-dibora-*s*-indacene-4,8-dione (3a). A mixture of phenylboronic acid **7a** (1.20 g, 10.0 mmol) and 2,3,5,6-tetraaminobenzoquinone **6** (504 mg, 3.0 mmol) in toluene (150 mL) was refluxed for 2 d. The resulting precipitate was filtered off while the solution was hot. Purification of the crude product by sublimation gave **3a** (194 mg, 19%) as a dark brown solid.

Mp > 400 °C (decomp.). MS/EI (70 eV): *m*/*z* 340 (M^+, 100%). IR(KBr) ν (cm^{-1}): 3463, 3339, 1621, 1506, 1400, 1247, 1148, 1017, 992, 746, 690. Anal. calcd for $C_{18}H_{14}B_2N_4O_2$: C, 63.60; H, 4.15; N, 16.48. Found: C, 63.38; H, 4.21; N, 16.37. HR-MS/EI: *m*/*z* (M^+): calcd for $C_{18}H_{14}B_2N_4O_2$ 340.1303. Found 340.1299.

2,6-Bis-(4-trifluoromethylphenyl)-2,3,6,7-tetrahydro-1*H*,5*H*-1,3,5,7-tetraaza-2,6-dibora-*s*-indacene-4,8-dione (3b). A mixture of 4-(trifluoromethyl)phenylboronic acid (1.00 g, 5.3 mmol) and 2,3,5,6-tetraaminobenzoquinone **6** (354 mg, 2.1 mmol) in toluene (150 mL) was refluxed for 36 h. The resulting precipitate was filtered off while the solution was hot. Purification of the crude product by sublimation gave compound **3b** (544 mg, 54%) as a dark brown solid.

Mp > 397 °C (decomp.). MS/EI (70 eV): *m*/*z* 476 (M^+, 100%). IR(KBr) ν (cm^{-1}): 3464, 3326, 1621, 1524, 1406, 1319, 1239, 1133, 1070, 1014, 833, 753, 660. Anal. calcd for $C_{20}H_{12}B_2F_6N_4O_2$: C, 50.47; H, 2.54; N, 11.77. Found: C, 50.24; H, 2.82; N, 11.73. HR-MS/EI: *m*/*z* (M^+): calcd for $C_{20}H_{12}B_2F_6N_4O_2$ 476.1051. Found 476.1043.

2,6-Bis-(4-phenylphenyl)-2,3,6,7-tetrahydro-1*H*,5*H*-1,3,5,7-tetraaza-2,6-dibora-*s*-indacene-4,8-dione (3c). A mixture of 4-phenylphenylboronic acid (2.00 g, 10.0 mmol) and 2,3,5,6-tetraaminobenzoquinone **6** (282 mg, 1.7 mmol) in toluene (150 ml) was refluxed for 36 h. The resulting precipitate was filtered off while the solution was hot. Purification of the crude product by sublimation gave compound **2** (26 mg, 4%) as a dark brown solid.

Mp > 400 °C (decomp.). MS/EI (70 eV): *m*/*z* 492 (M^+, 100%). IR(KBr) ν (cm^{-1}): 3459, 3313, 1633, 1523, 1401, 1330, 1244, 1152, 1015, 837, 765, 698, 660. Anal. calcd for $C_{30}H_{22}B_2N_4O_2$: C, 73.21; H, 4.51; N, 11.38. Found: C, 71.40; H, 4.31; N, 11.04. HR-MS/EI: *m*/*z* (M^+): calcd for $C_{30}H_{22}B_2N_4O_2$ 492.1929. Found 492.1938.

2,6-Bis-(4-*tert*-butylphenyl)-2,3,6,7-tetrahydro-1*H*,5*H*-1,3,5,7-tetraaza-2,6-dibora-*s*-indacene-4,8-dione (3d). A mixture of 4-*tert*-butylphenylboronic acid **7d** (250 mg, 1.40 mmol) and 2,3,5,6-tetraaminobenzoquinone **6** (80.0 mg, 0.48 mmol) in toluene (150 ml) was refluxed for 36 h. The resulting precipitate was filtered off while the solution was hot. Purification of the crude product by sublimation gave compound **3d** (65.4 mg, 30%) as a dark brown solid.

Mp > 400 °C (decomp.). MS/EI (70 eV): *m*/*z* 452 (M^+, 100%). ^{1}H-NMR: (DMSO, ppm) δ = 9.68 (s, 2H, NH), 9.66 (s, 2H, NH), 7.91 (d, 4H, J = 7.8 Hz), 7.34 (d, 2H, J = 7.8 Hz), 1.27 (s, 18H). IR(KBr) ν (cm^{-1}): 3467, 3322, 2957, 1619, 1405, 1330, 1241, 1152, 1012, 996, 823, 760, 658. Anal. calcd for $C_{26}H_{30}B_2N_4O_2$: C, 69.06; H, 6.69; N, 12.39. Found: C, 68.91; H, 6.04; N, 12.49.

Device fabrication

Bottom-contact FET. Highly doped n^+-Si wafers were used as substrates, and a layer of 300 nm of silicon dioxide (SiO_2: grown by thermal oxidation) was used as a gate dielectric layer. Cr (10 nm)/Au (20 nm) was successively evaporated and photolithographically delineated to obtain source and drain electrodes. The interdigitated structure of the source–drain contacts determined a channel length of 25 μm and a channel width of 294 mm (6 mm × 49). Substrates were cleaned by acetone, 2-propanol and ozone for 20 min, and immersed in hexamethyldisilazane (HMDS) at rt for over 12 h to treat the surface. Organic semiconductor layers (500 Å) were deposited on the channel region by vacuum evaporation at a rate of 0.2–0.3 Å s^{-1} under a pressure of 10^{-5} Pa.

Top-contact FET. The SiO_2 gate dielectric was 200 nm thick. The organic semiconductor (300 Å) was deposited on the SiO_2 by vacuum evaporation at a rate of 0.1–0.2 Å s^{-1} under a pressure of 10^{-5} Pa. During the evaporation, the temperature of the substrate was maintained by heating a copper block on which the substrate was mounted. Au was used as source and drain electrodes and deposited on the organic semiconductor layer through a shadow mask with a channel width (W) of 1000 μm and a channel length (L) of 50 μm. Finally, the FET measurements were carried out at rt in a vacuum chamber (10^{-5} Pa) without exposure to air with Hewlett-Packard 4140A and 4140B models.

Mobilities (μ) were calculated in the saturation regime by the relationship: $\mu_{sat} = (2I_{DS}L)/[WC_{ox}(V_G - V_{th})^2]$ where I_{DS} is the source–drain saturation current: C_{ox} is the oxide capacitance. V_G is the gate voltage and V_{th} is the threshold voltage. The latter can be estimated as the intercept of the linear section of the plot of $(I_{DS})^{1/2}$ *vs.* V_G.

Acknowledgements

This work is supported by a Grant-in-Aid for Scientific Research (no. 19350092 and 22550162) from the Ministry of Education, Culture, by Sports, Science and Technology, Japan, and by the Global COE program "Education and Research Center for Emergence of New Molecular Chemistry". We thank Center for Advanced Materials Analysis, Technical Department, TIT for measurements of elemental analysis and MS.

Notes and references

1 (*a*) H. Usta, C. Risko, Z. Wang, H. Huang, M. K. Deliomeroglu, A. Zhukhovitskiy, A. Facchetti and T. J. Marks, *J. Am. Chem. Soc.*, 2009, **131**, 5586; (*b*) A. R. Murphy and J. M. J. Fréchet, *Chem. Rev.*, 2007, **108**, 1066; (*c*) C. R. Newman, C. D. Frisbie, D. A. da Silva Filho, J. L. Brédas, P. C. Ewbank and K. R. Mann, *Chem. Mater.*, 2004, **16**, 4436.
2 Y. Shirota, *J. Mater. Chem.*, 2000, **10**, 1.
3 (*a*) S. Yamaguchi, T. Shirasaka, S. Akiyama and K. Tamao, *J. Am. Chem. Soc.*, 2002, **124**, 8816; (*b*) C. D. Entwistle and T. B. Marder, *Angew. Chem., Int. Ed.*, 2002, **41**, 2927; (*c*) C. D. Entwistle and T. B. Marder, *Chem. Mater.*, 2004, **16**, 4574; (*d*) T. Agou, J. Kobayashi and T. Kawashima, *Chem.–Eur. J.*, 2007, **13**, 8051.
4 (*a*) W. Niu, B. Rambo, M. D. Smith and J. J. Lavigne, *Chem. Commun.*, 2005, 5166; (*b*) B. M. Rambo and J. J. Lavigne, *Chem. Mater.*, 2007, **19**, 3732; (*c*) D. N. Coventry, A. S. Batsanov, A. E. Goeta, J. A. K. Howard, T. B. Marder and R. N. Perutz, *Chem. Commun.*, 2005, 2172.
5 (*a*) F. Jäkle, *Coord. Chem. Rev.*, 2006, **250**, 1107; (*b*) N. Matsumi, K. Kotera, K. Naka and Y. Chujo, *Macromolecules*, 1998, **31**, 3155.
6 (*a*) H. Noguchi, K. Hojo and M. Suginome, *J. Am. Chem. Soc.*, 2007, **129**, 758; (*b*) S. Yamaguchi and A. Wakamiya, *Pure Appl. Chem.*, 2006, **78**, 1413; (*c*) T. Kojima, J.-i. Nishida, S. Tokito and Y. Yamashita, *Chem. Lett.*, 2008, **37**, 1122.
7 (*a*) L. Weber, *Coord. Chem. Rev.*, 2001, **215**, 39; (*b*) L. Weber, V. Werner, M. A. Fox, T. B. Marder, S. Schwedler, A. Brockhinke, H.-G. Stammler and B. Neumann, *Dalton Trans.*, 2009, 1339; (*c*) S. Maruyama and Y. Kawanishi, *J. Mater. Chem.*, 2002, **12**, 2245; (*d*) L. Weber, V. Werner, M. A. Fox, T. B. Marder, S. Schwedler, A. Brockhinke, H.-G. Stammler and B. Neumann, *Dalton Trans.*, 2009, 2823.
8 (*a*) I. Yamaguchi, B.-J. Choi, T.-A. Koizumi, K. Kubota and T. Yamamoto, *Macromolecules*, 2007, **40**, 438; (*b*) I. Yamaguchi, T. Tominaga and M. Sato, *Polym. Int.*, 2009, **58**, 17; (*c*) T. Kojima, D. Kumaki, J.-I. Nishida, S. Tokito and Y. Yamashita, *J. Mater. Chem.*, 2011, **21**, 6607.
9 (*a*) Q. Tang, Z. Liang, J. Liu, J. Xu and Q. Miao, *Chem. Commun.*, 2010, **46**, 2977; (*b*) N. Hayashi, T. Yoshikawa, T. Ohnuma, H. Higuchi, K. Sako and H. Uekusa, *Org. Lett.*, 2007, **9**, 5417; (*c*) Q. Miao, M. Lefenfeld, T.-Q. Nguyen, T. Siegrist, C. Kloc and C. Nuckolls, *Adv. Mater.*, 2005, **17**, 407; (*d*) M. Mamada, D. Kumaki, J.-i. Nishida, S. Tokito and Y. Yamashita, *ACS Appl. Mater. Interfaces*, 2010, **2**, 1303.
10 n-Type FET materials with four-coordinate borons have recently reported (*a*) Y. Sun, D. Rohde, Y. Liu, L. Wan, Y. Wang, W. Wu, C. Di, G. Yu and D. Zhu, *J. Mater. Chem.*, 2006, **16**, 4499; (*b*) K. Ono, J. Hashizume, H. Yamaguchi, M. Tomura, J.-i. Nishida and Y. Yamashita, *Org. Lett.*, 2009, **11**, 4326; (*c*) K. Ono, A. Nakajima, Y. Tsuji, T. Kinoshita, M. Tomura, J.-i. Nishida and Y. Yamashita, *Chem.–Eur. J.*, 2010, **16**, 13539.
11 T. Suzuki, H. Fujii, Y. Yamashita, C. Kabuto, S. Tanaka, M. Harasawa, T. Mukai and T. Miyashi, *J. Am. Chem. Soc.*, 1992, **114**, 3034.